High-energy detector calibration data for k_0-Neutron Activation Analysis

László Szentmiklósi[1], Boglárka Maróti[1], Dénes Párkányi[1], Ildikó Harsányi[1], Zsolt Révay[2]

[1]*Nuclear Analysis and Radiography Department, Centre for Energy Research, Hungarian Academy of Sciences, 29-33 Konkoly-Thege Miklós street, 1121 Budapest, Hungary. E-mail: szentmiklosi.laszlo@energia.mta.hu*

[2]*Heinz Maier-Leibnitz Zentrum (MLZ), Technische Universität München, Lichtenbergstraße 1 D-85747 Garching, Germany*

Abstract

In k_0-neutron activation analysis, HPGe detectors have to be calibrated up to about 3.1 MeV, in order to properly determine the Na, Ca and S content of analytes. Commercial radioactive sources cover the energy range only up to 2.2 MeV, but with activation in the reactor, additional high-energy gamma emitter radionuclides (Ga-72, Mn-56, In-116 and Na-24) can be produced. At a prompt-gamma activation analysis station, where the calibration is available up to 12 MeV, we derived accurate gamma-ray energies and relative intensities for these radionuclides and subsequently used them for broad energy-range efficiency and nonlinearity calibration of NAA detectors as well as a low-level counting station.

Keywords

k_0-neutron activation analysis, HPGe detector calibration, energy and intensity data, uncertainty budget

Introduction

In order to apply k_0-neutron activation analysis (NAA) [1] to elements forming radionuclides with high-energy gamma-lines, such as Na (E=2754.0 keV), Ca (E=3084.4 keV) and S (E=3103.4 keV) [2], accurate detector calibration [3] over a wide energy range is necessary. In practice, if there is a disagreement between high- and low-energy lines of a multi-line isotope, we tend to discard the high-energy line, even though it is well separated and has proper statistical precision. If the efficiency curve is extrapolated beyond the available experimental data points, significant bias and loss of precision can occur [4]. This has to be assessed in order to further improve the analytical merits of k_0-NAA. From the quality assurance point of view, there are formal requirements (ISO 9001, ISO 17025, GLP) to establish and regularly execute a procedure to keep all gamma spectrometers in service calibrated and document their performance indicators, such as peak width, efficiency and nonlinearity over time.

Commercially available radioactive sources cover the energy range well only up to about 2.2 MeV. Cyclotron-produced radioisotopes with high-energy gamma rays (produced via ^{56}Fe(p,n)^{56}Co, ^{66}Zn(p,n)^{66}Ga or ^{63}Cu(α,n)^{66}Ga reactions) are adequate for this purpose, and have literature data [5, 6], but they are expensive, decay significantly between two subsequent detector calibration campaigns ($T_{1/2}$=77 days and 9.5 hours) and often not generally available to the NAA community. With activation in the reactor, however, several radionuclides having high-energy gamma lines, such as ^{72}Ga, ^{56}Mn, ^{116}In and ^{24}Na, can be produced at low additional cost. The application of Ga [7] [8] [9] and In isotopes [10] for detector calibration is hindered so far by the insufficient general confidence in their nuclear data.

At a PGAA station, where the detector calibration is done on a routine basis up to 12 MeV with a precision of about 1% for efficiency and about 0.01 keV for energy measurement, one can find ideal conditions to derive energies and relative intensities for such high-energy gamma emitters [6]. In this paper we report about the recent experiments made at the

Budapest PGAA facility [11], to produce a coherent dataset of such nuclides and apply them for efficiency and nonlinearity calibration of other gamma spectrometers. In combination with Monte Carlo calculations, this could form a basis of a more advanced detector calibration procedure in NAA.

Theory

First we identified a reference source that has many lines over a broad energy range, has well-known literature data, and the source is well-characterized by the supplier. Our choice was a sealed Ra-226 radioactive source from Physikalisch-Technische Bundesanstalt (PTB), for which a high-quality evaluation in form of an IAEA recommendation [12] is available. After activating the targets in a vertical channel [13] to ensure the target is as point-like as possible, we measured the gamma lines of the activated targets in repeated runs at a PGAA station. Splitting the available counting time helps to check the self-consistency (internal vs. external uncertainties) and establish the uncertainty budget (statistical vs systematic uncertainties) of the results.

Peak areas, after correcting with the established PGAA efficiency [14], will give gamma-ray emission probabilities of useful peaks relative to the most intense peak. That can be used at an NAA detector in a relative way, there is no need to scale the emission probabilities to their absolute values by multiplying with a literature P_γ and involve the associated uncertainty. Peaks within and beyond an existing calibration range are needed to append them to the existing curve in Hypermet-PC or Hyperlab [15, 16] as relative data. The detailed workflow of the calibration data generation is as follows:

Relative intensities

We consider peak area ratios, i.e. the peak area of interest relative to the most intense peak of the same isotope, to get a number between (0…1]. If repeated runs are available (taken e.g. using a custom Genie 2000 script), we make weighted averages (WA) of these peak area ratios from the successive spectra (with consideration of the error propagation of independent estimates), and only afterwards involve the efficiency correction (a systematic

uncertainty), otherwise we underestimate the efficiency curve's contribution to the uncertainty budget. So we compute $R_i = \mathrm{WA}_s\left\{\frac{A_i}{A_0}\right\}$, for the i^{th} line of an isotope, through the s available spectra. This has only statistical uncertainty, that can serve as weights in weighted averaging and can be used to compute the propagated uncertainty, as well as the empirical standard deviation of the results. If these two values are in agreement, it indicates that the spectrometer is stable and the peak evaluation is adequate. Subsequently we obtain $I_i = \frac{R_i}{\varepsilon_{ratio,i}}$ to correct for the previously established PGAA efficiency. Here efficiency ratio [17, 18] is enough, i.e. the uncertainty attributed to certified activities of sources can be excluded. If the correlations between efficiencies at different energies of the same curve [17, 18] are properly taken into account, a very low uncertainty can be attained. Further, if the identical sources are counted at the PGAA and NAA detectors, the developed procedure falls back to ratios of peak areas measured at different spectrometers, therefore it is expected to be very reliable and accurate.

Peak energies

For energy-determination, we measure the activated target in presence of the reference source to determine the energies of its two calibration lines. We choose peak couples where the reference isotope's peak is next to, or close to an intense peak of our isotope of interest. Here the energies can be propagated to the peaks with unknown energies without much risk for a bias due to the nonlinearity. These two energies can be used to energy-calibrate the previously taken spectra and generate accurate energies for all other peaks, this time also including the non-linearity curve as mathematically described in the Appendix.

Experimental

0.029960 g of $NaOH.H_2O$, 0.020023 g of Ga_2O_3, and 0.014124g of Mn_2O_3 were activated for 60 seconds in the pneumatic rabbit facility of the Budapest NAA laboratory [13]. The thermal equivalent neutron flux was of 5.7×10^{13} $cm^{-2}s^{-1}$, $f = 37.9$, $\alpha = 0.003$, fast neutron flux was 4.48×10^{12} $cm^{-2}s^{-1}$, giving a few MBq activity from each target. After about 4-12 hours of cooling times they were transferred to the PGAA station for data acquisition. As

In has short half-life and high neutron capture cross-section, 0.09862 g of In foil could be already activated in the cold-neutron beamline of the PGAA station. Na, Mn are monoisotopic elements, whereas for Ga, the used cooling time allowed the ^{70}Ga to decay out ($T_{1/2}$=21.15 min) completely. For In, thanks to the four-hour long activation in the beam, the ^{116m}In was saturated, but the metastable ^{114}In ($T_{1/2}$=49.5 d) was not, whereas the cooling time allowed the short-lived components to decay, so only the lines from ^{116m}In with $T_{1/2}$=54 min were observed.

Given the solid angle of the PGAA detector is as low as 0.001, the true and the random coincidence summing could be avoided and the count rate could be kept moderate to maintain the well-fittable peak shapes, in order to generate calibration energy and intensity data. At least four spectra were taken at the PGAA spectrometer for each target using batch data acquisition. The decay spectra were analyzed with the Hypermet-PC software [19, 20].

Later, to facilitate the detector calibration step, the same sources (from the same irradiation or re-activated later under identical conditions), in addition to the standard set of commercial calibration sources (^{241}Am, ^{133}Ba, ^{207}Bi, ^{60}Co, ^{137}Cs, ^{152}Eu, ^{226}Ra) were counted with a 13% n-type HPGe and a Canberra DSA-2000 spectrometer at 235 mm distance in the DÖME low-level counting and in-beam activation analysis station [11, 21], and also with the D4 (36% n-type HPGe) and D5 (55% p-type HPGe) detectors of the NAA laboratory at 300 mm distances, using an Ortec DSPEC 502 spectrometer in ZDT mode. The energy range of the MCA histogram was set from 20 keV to 3.5 MeV. In case of the DÖME we still used Hypermet-PC program for spectroscopy, whereas for D4 and D5 the more recent Hyperlab.

Results and discussion

Energy calibration and relative intensity data

Using the procedure described above, the energies of calibration two peaks for each the neutron-activated sources were determined, using the Ra-226 reference source. The results are listed in Table 1.

Table 1 Energy-calibration transfer peaks of the four radionuclides

Nuclide	Calibration transfer peaks of ^{226}Ra (keV) [12]	Measured calibration transfer peak energies of the relevant nuclide (keV)
Ga-72	609.316 ± 0.003 2204.071 ± 0.021	600.910 ± 0.003 2201.529 ± 0.036
In-116	806.185 ± 0.011 2118.536 ± 0.008	818.625 ± 0.018 2112.073 ± 0.031
Mn-56	806.185 ± 0.011 2118.536 ± 0.008	846.741 ± 0.022 2113.029 ± 0.031
Na-24	1377.669 ± 0.012 2447.673 ± 0.010	1368.591 ± 0.020 2754.016 ± 0.040

These data were applied as calibration energies in order to derive the energies of all other peaks from spectra without the reference source. It is to note that due to decay during counting, the subsequent spectra have decreasing peak areas, i.e. decreasing statistical precision of peak positions and intensities, so for each quantity, weighted average shall be used instead of the arithmetic average. The MCA histograms shall be cleared in between the restarts to maintain the statistical independence of the recorded counts. Positions of

each peak in each spectrum are translated to energy domain individually using formulae described in the Appendix.

Table 2 is to illustrate the uncertainty budget for the 894-keV line of Ga-72 based on successively recorded spectra. One can see that the data we obtained for peak positions using Hypermet-PC are well under statistical control. Internal uncertainty is from the error propagation of independent variables, whereas external uncertainty is obtained from the empirical scattering of data points. Statistical uncertainty is only influenced by the counting statistics whereas systematic uncertainty, the dominating part of the quoted total uncertainties, comprises the contributions of the energy calibration data (see Table 1), the nonlinearity, i.e. all quantities that cannot be reduced by prolonging the counting time.

Table 2 Statistical consistency of nine repeated runs of two hours each for the 894-keV line of Ga-72.

Run No.	Position 894 keV (ch)	Abs. Unc.	Position 601 keV (ch)	Unc	Position 2201 keV (ch)	Unc	Energy (keV)	Total Unc	Statistical Unc	Systematic Unc
1	1238.541	0.008	829.707	0.007	3061.22	0.008	894.250	0.023	0.007	0.022
2	1238.56	0.007	829.724	0.011	3061.252	0.01	894.250	0.023	0.008	0.022
3	1238.554	0.007	829.734	0.008	3061.235	0.01	894.242	0.023	0.007	0.022
4	1238.575	0.007	829.755	0.009	3061.234	0.009	894.245	0.023	0.007	0.022
5	1238.57	0.009	829.744	0.007	3061.247	0.011	894.246	0.023	0.009	0.022
6	1238.564	0.008	829.752	0.01	3061.255	0.01	894.236	0.023	0.008	0.022
7	1238.585	0.01	829.765	0.009	3061.318	0.013	894.235	0.024	0.010	0.022
8	1238.596	0.011	829.74	0.013	3061.372	0.012	894.250	0.024	0.011	0.022
9	1238.596	0.01	829.737	0.014	3061.366	0.014	894.253	0.024	0.011	0.022

Weighted average	894.245
Internal statistical unc	0.003
External statistical unc	0.002
Total uncertainty	0.022

The generated calibration data for all four radionuclides are summarized in Table 3. For Mn-56 and Na-24, where the nuclear data in the literature are already accurate [12] [22], we were able to confirm them and reproduce them, giving a confidence that our overall procedure is adequate for the two other nuclides of interest as well. In general, the

uncertainties of the data are sufficiently low to apply them in gamma spectrometry of instrumental k_0-NAA.

Table 3 Measured calibration energies and relative intensities of the four radionuclides. Tabulation does not list all known transitions, only the practically useful gamma lines. Literature data: ^{56}Mn, ^{24}Na: Ref. [22], ^{116}In: Ref. [10] ^{72}Ga: Ref. [7]

Energy (keV)	Unc.	Literature Energy (keV)	Literature Unc (keV)	Relative emission probability	Unc.	Literature relative emission probability	Literature Unc
^{56}Mn							
846.741	0.022	846.764	0.0019	1		1	
1810.67	0.029	1810.73	0.004	0.2665	0.0013	0.272	0.004
2113.03	0.036	2113.09	0.006	0.1418	0.0008	0.143	0.003
2522.79	0.051	2523.06	0.05	0.01019	0.00017	0.01032	0.00020
2657.39	0.054	2657.56	0.004	0.00682	0.0001	0.00653	0.00007
2959.78	0.066	2959.92	0.01	0.00316	0.00007	0.00311	0.00005
3369.64	0.08	3369.84	0.04	0.00205	0.00005	0.00172	0.00010
^{24}Na							
1368.59	0.02	1368.63	0.005	1		1	
2754.02	0.04	2754.01	0.011	0.993	0.012	0.999	0.0008
^{116}In							
138.316	0.015	138.326	0.008	0.0419	0.0005	0.0390	0.0014
355.411	0.015	355.36	0.04	0.0086	0.0002	0.0098	0.0005
416.873	0.004	416.86	0.03	0.3306	0.0028	0.328	0.014
463.198	0.007	463.14	0.12	0.0089	0.0002	0.0098	0.0006
818.625	0.019	818.7	0.2	0.1457	0.0013	0.136	0.0005
972.5	0.024	972.4	0.2	0.0057	0.0002	0.00538	0.00019
1097.17	0.019	1097.3	0.2	0.6906	0.0049	0.666	0.013
1293.49	0.031	1293.54	0.21	1		1	
1507.49	0.005	1507.4	0.2	0.1168	0.001	0.118	0.004
1752.34	0.012	1753.8	0.6	0.028	0.0004	0.0291	0.009
2112.07	0.031	2112.1	0.4	0.1798	0.0017	0.184	0.005
^{72}Ga							
600.910	0.008	600.916	0.012	0.06155	0.00038	0.0613	0.0005

629.955	0.008	600.979	0.012	0.2741	0.0017	0.2738	0.0020
786.427	0.008	786.529	0.012	0.03531	0.00003	0.03532	0.00016
810.255	0.009	810.355	0.012	0.02204	0.00006	0.02201	0.00010
834.074	0.009	834.170	0.012	1		1	
894.250	0.01	894.336	0.012	0.10594	0.00031	0.1063	0.0004
970.672	0.011	970.772	0.012	0.01153	0.00002	0.01163	0.0006
999.893	0.012	999.995	0.012	0.00847	0.00002	0.00851	0.00004
1050.694	0.013	1050.800	0.012	0.07273	0.00009	0.0732	0.0004
1215.098	0.016	1215.139	0.013	0.0085	0.00003	0.00863	0.00006
1230.901	0.016	1230.934	0.013	0.01501	0.00003	0.01513	0.0001
1260.094	0.017	1260.124	0.013	0.01224	0.00003	0.01244	0.00008
1276.773	0.017	1276.798	0.013	0.01666	0.00004	0.01669	0.00011
1463.994	0.021	1464.054	0.014	0.03768	0.00007	0.03763	0.00031
1568.163	0.027	1568.071	0.020	0.00181	0.00003	0.001739	0.000024
1571.618	0.024	1571.600	0.014	0.00883	0.00003	0.00897	0.00009
1596.756	0.024	1596.735	0.014	0.04544	0.00009	0.0458	0.0004
1680.70	0.026	1680.741	0.015	0.00962	0.00004	0.00960	0.00010
1710.846	0.027	1710.33+ 1711.17*	0.08	0.00464	0.00002	0.0046	0.0007
1837.102	0.031	1837.148	0.019	0.00227	0.00002	0.00231	0.00004
1860.980	0.03	1860.990	0.016	0.05693	0.00013	0.0567	0.0007
1877.688	0.037	1877.680	0.019	0.00232	0.00002	0.00244	0.00004
1920.227	0.034	1920.226	0.024	0.00179	0.00002	0.00176	0.00004
2109.331	0.036	2109.356	0.017	0.01136	0.00004	0.01147	0.00017
2201.529	0.038	2201.582	0.017	0.284	0.0006	0.282	0.005
2214.001	0.039	2214.022	0.020	0.00241	0.00002	0.00241	0.00004
2490.929	0.044	2491.029	0.018	0.08178	0.00019	0.081	0.002
2507.605	0.045	2507.714	0.018	0.14035	0.00031	0.140	0.003
2514.720	0.046	2514.857	0.019	0.00326	0.00003	0.00334	0.00007
2621.113	0.049	2621.281	0.023	0.00152	0.00001	0.00150	0.00004
2844.018	0.053	2844.171	0.035	0.00458	0.00003	0.00467	0.00013
2939.855	0.074	2940.19	0.06	0.00015	4E-06	0.000154	0.000006
2981.292	0.058	2981.50	0.05	0.00063	8E-06	0.000643	0.000021
3035.440	0.064	3035.52	0.06	0.00025	5E-06	0.000201	0.000008
3067.405	0.111	3067.32	0.11	3.9E-05	3E-06	0.000038	0.000003
3094.232	0.067	3094.39	0.10	0.00018	4E-06	0.000170	0.000006
3324.869	0.099	3325.35	0.11	9.7E-05	4E-06	0.000081	0.000005

3337.854	0.162	3338.55	0.15	4.7E-05	3E-06	0.000047	0.000004

*: sum of a doublet from Ref [6].

Application to broad-energy detector calibration

The data could be imported to Hypermet PC via the nuclid.std file, and to Hyperlab via its custom nuclear data import feature. The sources were counted at the NAA spectrometers D4 and D5, as well as the DÖME station located next to the PGAA beamline. Care was taken to measure the sources at the farthest available distance, where true coincidence summing was found to be negligible. The resulting nonlinearity and efficiency calibration curves are illustrated in Figs. 1 and 2, up to about 3.3 MeV energies.

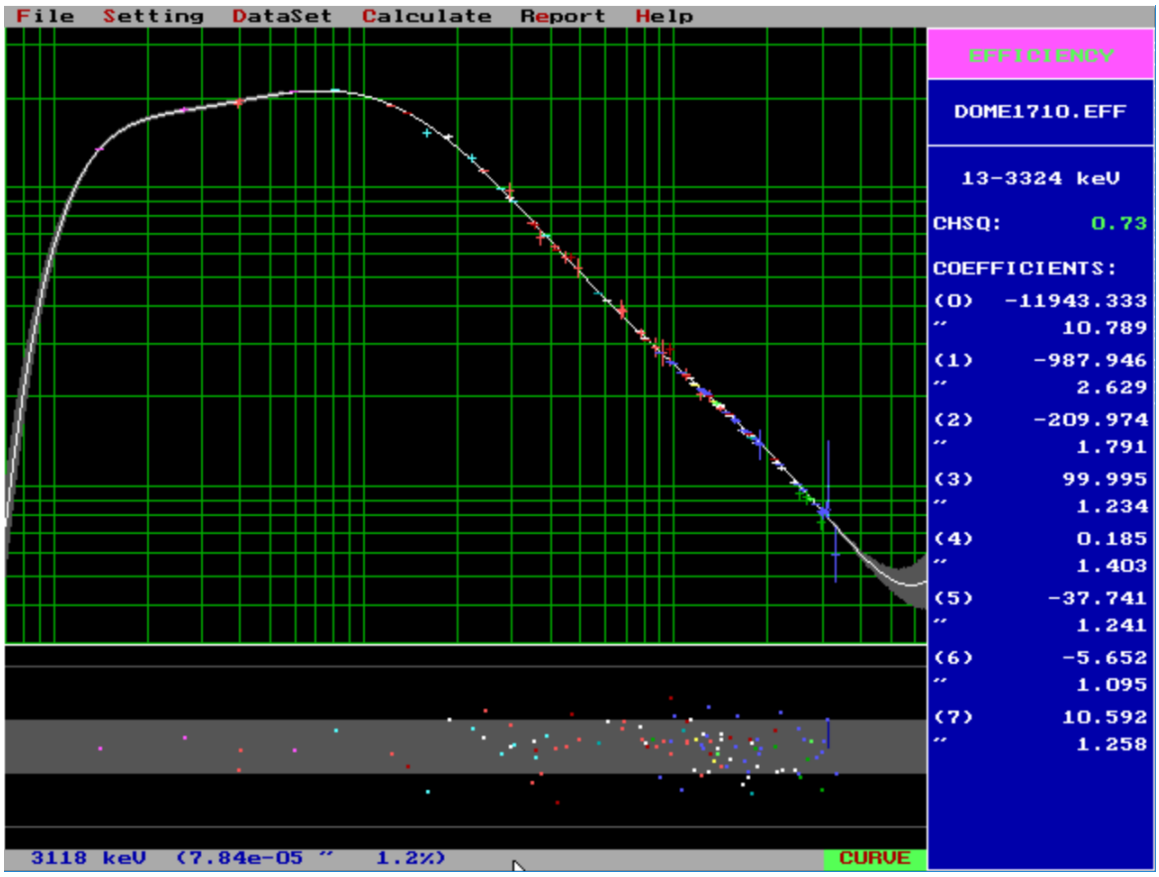

Figure 1: the efficiency curve of the DÖME spectrometer up to 3.3 MeV, displayed in log-log scale.

Figure 2: the nonlinearity curve of the DÖME spectrometer when used in energy range up to 3.5 MeV. The horizontal axis is the peak position (in channel units) whereas the vertical axis is the corresponding deviation from the linear energy-channel calibration model (also in channels)

It was concluded that at 3.1 MeV, where Ca and S lines are present in NAA, the value of the efficiency curve differs only slightly, and remains within the uncertainty range from the extrapolated old efficiency curve, indicating that Ra-226 was already useful to define the trend of the efficiency curve. This also confirms that our previous analysis results were correct, but probably with somewhat higher assigned uncertainty. However, the 25-30 additional points at the high-end of the curve highly reduces its uncertainty (e.g. $7.84\times10^{-5} \pm 5.0\%$ vs. $7.74\times10^{-5} \pm 1.2\%$ for DÖME counting station, $1.55\times10^{-4} \pm 4.1\%$ vs. $1.60\times10^{-4} \pm 0.6\%$ for the D4 NAA detector). Transfer to any closer geometry can be facilitated using single-line sources, e.g. Cs-137, the Kayzero/Solcoi [23] or EFFTRAN

[24] software, or via Monte Carlo calculations for unconventional sample shapes and geometries [25].

Conclusions

It was demonstrated that a prompt-gamma activation analysis spectrometer with its well-established high-energy calibration can refine and extend the present calibration practice used in k_0-NAA. To facilitate this, a coherent set of energies and relative emission intensities traceable to Ra-226 were determined experimentally at the Budapest PGAA station for Na-24, Mn-56, Ga-72 and In-116, and were applied to the efficiency and nonlinearity of three other HPGe spectrometers. As a result, our NAA and in-beam NAA/environmental counting stations are now well-calibrated within the entire required energy range, from 20 keV to 3.3 MeV with a precision better than 1-2%. Mathematical background and uncertainty budget of the entire computation are clarified and presented. We expect that such harmonization of efficiency- and nonlinearity-calibration approaches will ultimately resolve some known ambiguities and discrepancies in the k_0-data, and in particular, will improve the accuracy of the daily neutron activation analysis results for elements Ca, S, and Na.

Acknowledgements

The first author gratefully acknowledges the financial support of the Bólyai János Research Fellowship of the Hungarian Academy of Sciences. This work was part of the project No. 127102 that has been implemented with the support provided from the National Research, Development and Innovation Fund of Hungary, financed under the NN_17 V4-Korea funding scheme.

References

1. De Corte F (1987) The k_0-standardization method. Rijksuniversiteit Gent, Gent

2. Jacimovic R, De Corte F, Kennedy G, et al (2014) The 2012 recommended k(0) database. J Radioanal Nucl Chem 300:589–592.

3. Moens L, De Corte F, Simonits A, et al (1982) Calculation of the absolute peak efficiency of Ge and Ge(Li) detctors for different counting geometries. J Radioanal Nucl Chem 70:539–550.

4. Kučera J, Kubešová M, Lebeda O (2017) Improvement of the Ca determination accuracy with k0-INAA using an HPGe coaxial detector with extended energy range efficiency calibration. J. Radioanal. Nucl. Chem. in press:

5. Barker PH, Connor RD (1967) ^{56}Co as a calibration source up to 3.5 MeV for gamma ray detectors. Nucl Instr Method 57:147–151.

6. Baglin CM, Browne E, Norman EB, et al (2002) Ga-66: a standard for high-energy calibration of Ge detectors. Nucl Instruments Methods Phys Res Sect a- Accel Spectrometers Detect Assoc Equip 481:365–377.

7. Medeiros JA., Zamboni CB, Lapolli AL, et al (2001) Decay of 72-Ga. Appl Radiat Isot 54:245–259. doi: 10.1016/S0969-8043(99)00282-1

8. Rester AC, Ramayya A V, Hamilton JH, et al (1971) Levels in 72Ge populated by 72Ga. Nucl Phyics A 162:461–480.

9. Koskinas MF, Moreira DS, Takeda MN, et al (2006) Primary standardization of 72Ga. Appl Radiat Isot 64:1225–1228.

10. Blachot J, Marguier G (1994) Nuclear Data Sheets for A=116. Nucl Data Sheets 73:81.

11. Szentmiklósi L, Belgya T, Révay Z, Kis Z (2010) Upgrade of the prompt gamma activation analysis and the neutron-induced prompt gamma spectroscopy facilities at the Budapest research reactor. J Radioanal Nucl Chem. 286: 501-505 doi: 10.1007/s10967-010-0765-4

12. Bé MM, Chechev VP, Dersch R, et al (2007) Update of X-ray and gamma ray decay data standards for detector calibrations and other applications, STI/PUB/1287, Volume 1. IAEA, Vienna

13. Szentmiklósi L, Párkányi D, Sziklai-László I, (2016) Upgrade of the Budapest neutron activation analysis laboratory. J Radioanal Nucl Chem 309:91–99. doi: 10.1007/s10967-016-4776-7

14. Molnár GL, Révay Z, Belgya T, et al (2002) Wide energy range efficiency calibration method for Ge detectors. Nucl Instruments Methods Phys Res Sect a-Accel Spectrometers Detect Assoc Equip 489:140–159.

15. Fazekas B, Östör J, Kiss Z, et al (1998) Quality assurance features of "HYPERMET-PC." J Radioanal Nucl Chem 233:101–103.

16. Simonits A, Östör J, Kálvin S, Fazekas B (2003) HyperLab: A new concept in gamma-ray spectrum analysis. J. Radioanal. Nucl. Chem. 257:589–595

17. Belgya T (2014) Uncertainty calculation of functions of γ-ray detector efficiency and its usage in comparator experiments. J Radioanal Nucl Chem 300:559–566.

18. Révay Z (2006) Calculation of uncertainties in prompt gamma activationanalysis. Nucl Instruments Methods Phys Res Sect a- Accel Spectrometers Detect Assoc Equip A 564:688–697.

19. Fazekas B, Molnár G, Belgya T, et al (1997) Introducing HYPERMET-PC for automatic analysis of complex gamma-ray spectra. J Radioanal Nucl Chem 215:271–277.

20. Fazekas B, Belgya T, Dabolczi L, et al (1996) HYPERMET-PC: Program for automatic analysis of complex gamma- ray spectra. J Trace Microprobe Tech 14:167–172.

21. Kis Z, Völgyesi P, Szabó Z (2013) DÖME: Revitalizing a low-background counting chamber and developing a radon-tight sample holder for gamma-ray spectroscopy measurements. J Radioanal Nucl Chem 298:2029–2035.

22. Bé M-M, Christé V, Dulieu C, et al (2004) Table of Radionuclides, Vol. 1 - A = 1 to 150, Monographie BIPM-5.

23. De Corte F, Van Sluijs R, Simonits A, et al (2001) Installation and calibration of Kayzero-assisted NAA in three Central European countries via a Copernicus project. Appl Radiat Isot 55:347–354. doi: 10.1016/S0969-8043(01)00063-X

24. Vidmar T (2005) EFFTRAN - A Monte Carlo efficiency transfer code for gamma-ray spectrometry. Nucl Instruments Methods Phys Res Sect A Accel Spectrometers, Detect Assoc Equip 550:603–608. doi: 10.1016/j.nima.2005.05.055

25. Szentmiklósi L, Belgya T, Maróti B, Kis Z (2014) Characterization of HPGe gamma spectrometers by geant4 Monte Carlo simulations. J Radioanal Nucl Chem. 300:553-558 doi: 10.1007/s10967-014-2976-6

Appendix

Let us consider two calibration peaks (with indices 1 and 2) in a gamma spectrum with positions P (in units of channel) and known literature energies E (e.g. in keV) and define quantity, a couple of a value (v) and its corresponding 1-sigma uncertainty (δ), as follows: $P_1 := (P_1, \delta P_1)$, $P_2 := (P_2, \delta P_2)$, $E_1 := (E_1, \delta E_1)$, $E_2 := (E_2, \delta E_2)$. Further, we define P_0, an internal variable, as the average of the two calibration positions:

$$P_0 := \frac{P_1 + P_2}{2} = \left(\frac{1}{2}(P_1 + P_2), \frac{1}{2}\sqrt{\delta P_1^2 + \delta P_2^2}\right)$$

If we look for the linear energy calibration in a form of $E = a + b(P - P_0)$ and solve the system of equations for a and b, we get:

$$a = \left(\frac{1}{2}(E_1 + E_2), \frac{1}{2}\sqrt{\delta E_1^2 + \delta E_2^2}\right)$$

$$b = \left(\frac{E_1 - E_2}{P_1 - P_2}, \sqrt{\frac{(E_1 - E_2)^2\,\delta P_1^2}{(P_1 - P_2)^4} + \frac{(E_1 - E_2)^2 \delta P_2^2}{(P_1 - P_2)^4} + \frac{\delta E_1^2}{(P_1 - P_2)^2} + \frac{\delta E_2^2}{(P_1 - P_2)^2}}\right)$$

These a and b are different for each repeated run as, especially the offset component of the energy calibration and to a much less extent the gain, changes slightly at each clear of MCA memory. Term a is only systematic, as it contains only literature energies, whereas b contains statistical (δP) and systematic components (δE).

For a third peak in between P_1 and P_2, with fitted position P_3, where the nonlinearity is non-zero (N_3), E_3 becomes:

$$E_3 = \frac{1}{2}(E_1 + E_2) + \frac{(E_1 - E_2)\left(P_3 + N_3 - \frac{1}{2}P_1 - \frac{1}{2}P_2\right)}{P_1 - P_2}$$

$$\delta E_3 = \frac{1}{2} sqrt\left[\begin{array}{c} \frac{4(E_1 - E_2)^2 \left(\frac{1}{4}\delta P_1^2 + \frac{1}{4}\delta P_2^2\right)}{(P_1 - P_2)^2} + \delta E_1^2 + \delta E_2^2 + \\ 4\left(P_3 + N_3 - \frac{1}{2}P_1 - \frac{1}{2}P_2\right)^2 \left(\frac{(E_1 - E_2)^2 \delta P_1^2}{(P_1 - P_2)^4} + \frac{(E_1 - E_2)^2 \delta P_2^2}{(P_1 - P_2)^4} + \frac{\delta E_1^2}{(P_1 - P_2)^2} + \frac{\delta E_2^2}{(P_1 - P_2)^2}\right) + \\ \frac{4(E_1 - E_2)^2 \delta N_3^2}{(P_1 - P_2)^2} + \frac{4(E_1 - E_2)^2 \delta P_3^2}{(P_1 - P_2)^2} \end{array} \right]$$

The related variance, i.e. the square of δE_3, can be decomposed to statistical and systematic components:

$$\Delta E_{3,stat} = \frac{(E1 - E2)^2 \left(\frac{1}{4}\delta P1^2 + \frac{1}{4}\delta P2^2\right)}{(P1 - P2)^2} + \frac{(E1 - E2)^2 \delta P3^2}{(P1 - P2)^2} + \left(P3 + N3 - \frac{1}{2}P1 - \frac{1}{2}P2\right)^2 \left(\frac{(E1 - E2)^2 \delta P1^2}{(P1 - P2)^4} + \frac{(E1 - E2)^2 \delta P2^2}{(P1 - P2)^4}\right)$$

$$\Delta E_{3,syst} = \frac{1}{4}\delta E1^2 + \frac{1}{4}\delta E2^2 + \left(P3 + N3 - \frac{1}{2}P1 - \frac{1}{2}P2\right)^2 \left(\frac{\delta E1^2}{(P1 - P2)^2} + \frac{\delta E2^2}{(P1 - P2)^2}\right) + \frac{(E1 - E2)^2 \delta N3^2}{(P1 - P2)^2}$$